Design and Non-Linear Modeling of a Wide Tuning Range Four-Plate MEMS Varactor with High Q-Factor for RF Application

M. Moradi [1], R. S. Shirazi [1], and A. Abdipour [2]

[1] Microwave Measurement Lab., Department of Electrical Engineering
[2] Institute of Communication Technology & Applied Electromagnetics
Amirkabir University of Technology (Tehran Polytechnic), Tehran, 158754413, Iran
mehrdad_moradi@aut.ac.ir, sarraf@aut.ac.ir, abdipour@aut.ac.ir

Abstract ─ In this study, a micro-electromechanical variable capacitor that can achieve a wide tuning range is presented. The mechanical behaviors such as squeezed film damping and modal analysis are investigated. Also, scattering parameters, electromagnetic properties, and linear and nonlinear circuit models are presented for MEMS varactors. The four-plate tunable capacitor has nominal capacitance of 0.055 pF, a Q-factor of 175 at 10 GHz, and a tuning range of 2.59:1. The presented four-plate MEMS varactor has a suspended plate with the ability of moving downward and upward in order to increase the tuning range. The results were obtained by using simulation software. For the mechanical analyses, FEM in COMSOL Multiphysics software was used, and Ansoft HFSS and Agilent ADS were used for the electromagnetic analyses.

Index Terms ─ Linear model, MEMS varactor, nonlinear model, tuning range.

I. INTRODUCTION

In wireless communication systems, VCOs and tunable filters need high quality factor components. This can lead to low phase noise and low power in voltage-controlled oscillators (VCO) and low insertion loss in the band pass filters. High quality factor variable capacitors (varactors) with common p-n junction are off-chip [1,2]. There are problems with off-chip passive components such as packaging complexity, high cost and large system area. These problems have increased the need for a new technology to realize high performance on-chip passive elements which can be monolithically integrated with active circuitry.

Recent investigations into micromachining proposed RF MEMS (microelectromechanical system) varactors with an adequate Q-factor. MEMS varactors are fabricated in either an aluminum [3] or a polysilicon [4] surface micromachining technology. MEMS varactors provide high quality factor, wide tuning range, low phase noise and small chip size and are compatible with the standard IC fabrication [5-8]. MEMS varactors

have a high Q-factor and wide tuning range due to the unique capabilities enabled by micromechanical tuning and the low loss materials used in the construction of RF MEMs devices. Since their mechanical resonance frequency is normally around 10-100 KHz, the MEMS varactors will not resonate mechanically in response to the RF frequencies.

Parallel plate configuration of MEMS varactors is the most common configuration that has been used because of its simplicity in fabrication and high Q-factor. The parallel plate MEMS varactors consist of a suspended metal plate over a bottom fixed metal plate. By applying a DC voltage between two plates, the suspended metal plate moves toward the bottom plate, and this being the case, displacement between two plates results in the variation of the capacitance. A two parallel plate MEMS varactor with a Q-factor on the order of 60 and a measured tuning range of 16% were reported in [3]. It was shown that the measured tuning range of MEMS varactors are less than their theoretical calculation. The foremost limitation of MEMS varactors is their actual tuning range being less than their theoretical one. To overcome this problem, Young et al. [3], Dec et al. [4], and Chen et al. [11] have offered some solutions and innovative efforts. Furthermore, a different structure with seven supporting beams is presented in [16], which its capacitance ranges from 0.064pF for a single beam structure to 0.448 pF for a seven beam structure.

This paper presents a four parallel plate MEMS varactor that offers a large tuning range on the order of 2.59:1 with a high Q-factor of 175 at 10 GHz. For mechanical and electrostatic calculation, we used COMSOL Multiphysics 3.5a. The electromagnetic behaviors were simulated by Ansoft HFSS and Agilent ADS. A linear circuitry model is proposed by scattering parameters extracted from HFSS simulation outcomes. Finally, a new nonlinear circuitry model was prepared for MEMS varactors devices. Using this nonlinear circuitry model in circuit simulators to simulate circuits consisting MEMS varactors is possible. Only by

changing some input parameters of the model, the nonlinear model can be applied to RF MEMS varactors. The principle of its operation is described in Section II. The varactor design including electrostatic activation, pull-in effect, computation of spring constant, squeezed film damping and modal analysis is discussed in Section III. The static electrostatic analysis and electromagnetic simulation are presented in Section IV and V, respectively, and finally, the linear and nonlinear circuitry models are elaborated in Section VI.

II. PRINCIPLE OF OPERATION

A two parallel plate MEMS varactor is shown in Fig. 1. The top plate is suspended by cantilever beams and the bottom metal plate is fixed. The overlapping area and the initial spacing between the two plates are called A and d_0, respectively. When a bias voltage is applied across the two plates, it induces an electrostatic force on them and causes the suspended plate to move towards the bottom plate until the electrostatic and spring forces become equal. This displacement increases the value of the capacitance.

The value of the capacitance (C) between two plates can be calculated by the following equation:

$$C = \frac{\varepsilon A}{d}, \qquad (1)$$

where d is the distance between two plates. If V_{DC} is applied across the two plates, an attractive electrostatic force is generated between them. The electrostatic force can be derived as [9,10]:

$$F_e = \frac{1}{2}\frac{\partial C(d)}{\partial d}V_{DC}^2 = -\frac{1}{2}\frac{\varepsilon_0 A V_{DC}^2}{d^2}, \qquad (2)$$

where A is the overlapping surface between the two plates. The suspended plate moves downward to reach an equilibrium between electrostatic force and the mechanical restoring force. The mechanical restoring force is given by Equation (3), where k_m is the spring constant of the suspended plate. By equating these two forces, we find:

$$\frac{1}{2}\frac{\varepsilon_0 A V_{DC}^2}{h^2} = k_m(d_0 - d). \qquad (3)$$

Increasing applied voltage leads to decrease distance between top and bottom plates until d reaches $d_0/3$. The corresponding voltage at $d=d_0/3$ is called pull-in voltage. If V_{DC} increases beyond pull-in voltage, the suspended plate collapses down onto the bottom plate at $d=2d_0/3$. The increase in the electrostatic force is greater than the increase in the restoring force and no equilibrium position can be reached between the two forces; consequently, the suspended beam position becomes unstable. This event is called pull-in effect. Pull-in effect limits capacitance tuning range to 1.5:1. To solve this problem, a new design is proposed in [11].

Presented in [11], Fig. 2, illustrates the novel design

of two parallel MEMS capacitor. As shown in Fig. 2, the plate E_1 is a suspended plate with the ability of moving down. E_2 and E_3 are fixed on the bottom substrate. In this design, actuated beams and capacitor beams are separated. E_1 and E_2 form a variable capacitor. The electrostatic actuation is provided by plate E_3 (the plate that surrounds E_2) and E_1. The distance between E_1 and E_2 that is called d_1 is designed to be smaller than d_2. Pull-in effect occurs between plates E_1 and E_3 at $d=d_2/3$ that makes further change in the capacitance between E_1 and E_2. The relative tuning range is calculated by:

$$\frac{C - C_0}{C_0} = \frac{\varepsilon A/(d_1 - d) - \varepsilon A/d_1}{\varepsilon A/d_1} = \frac{d}{d_1 - d}. \qquad (4)$$

When d reaches $d_2/3$, the maximum tuning range can be obtained. Replacing d with $d_2/3$ in Equation (4) results in a maximum tuning range of $d_2/(3d_1-d_2)$. By choosing $d_1=2~\mu m$ and $d_2=3~\mu m$ in [11], the tuning range of 1:1 is achieved.
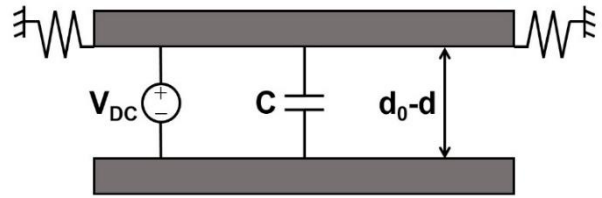

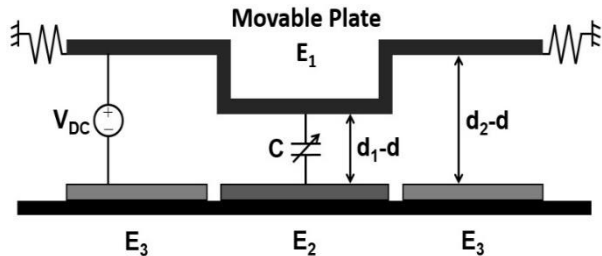Fig. 1. Cross-section of two-parallel plate micromachined varactor.

Fig. 2. A schematic model of the MEMS tunable capacitor using different gap spacing [11].

III. A NEW DESIGN OF THE PARALLEL PLATE MEMS VARACTOR

Using the configuration idea presented in [11] and [5], we achieved a novel design that increases the tuning range of the three plate varactor proposed in [11]. Figure 3 illustrates schematic model of our design. The fourth plate (E_4) is used to move the suspended plate (E_1) upward. The 3D configuration and career beams of E_1 are shown in Fig. 4. When a bias voltage is applied between E_1 and E_4, electrostatic force is generated on plates and E_1 moves toward E_4. E_4 is suspended by high stiffness beams and its displacement due to the applied voltage can be neglected. When the biasing voltage is

applied between E_1 and E_3, the maximum value of capacitance will be $\varepsilon A/(d_1-d_2/3)$. Due to the DC voltage applied across E_1 and E_4, E_1 moves upward and capacitance value decreases until pull-in effect occurs between E_1 and E_4. The minimum value of capacitance is derived as $\varepsilon A/(d_1+d_2/3)$. By choosing d_1 and d_2 as in [11] and $d_3=2$ μm, tuning range of 3:1 is accomplished. It must be noticed that this wide tuning range is completely controlled by biasing voltage. Another advantage of adding E_4 to the structure is protecting other plates using a firm and bulky plate. Gold is chosen for E_1, E_2 and E_3. Nickel for E_4, and silicon for substrate. Plates E_1 and E_4 thickness are respectively *2* and *15 µm*. Plates E_2 and E_3 thickness is *0.5 µm*, which can be thermally evaporated on the substrate. Silicon with *1 mm* thickness is used as the substrate.
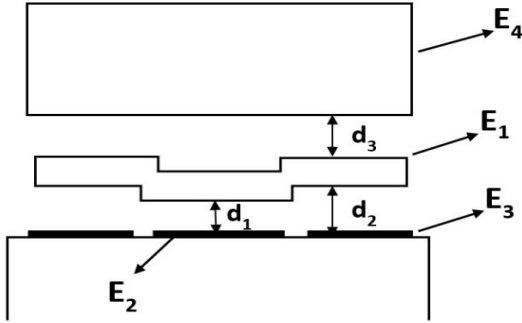

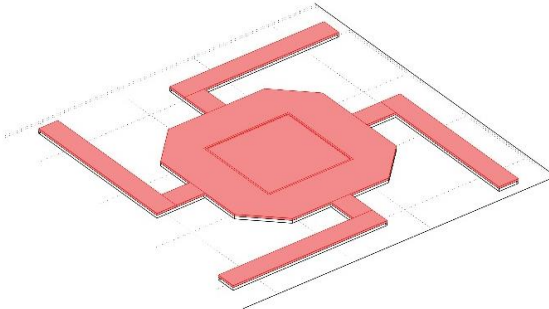Fig. 3. A schematic model of the novel wide-tuning-range tunable capacitor.

Fig. 4. The suspended plate E_1 and its beams.

IV. STATIC ELECTROMECHANICAL SIMULATION

Electrical and mechanical physical domains must be considered among simulation of RF MEMS devices. Accordingly, the relation between electrical and mechanical parameters should be taken into account. The simulations, were performed in a 3D domain, and used the finite element method (FEM) in the COMSOL Multiphysics 3.5a.

Career beams of E_1 plate are designed in order to make tradeoff between low control voltage and low

sensitivity due to the external forces. E_1 spring coefficient is 6.5 which is calculated by simulation. Pull-in effect between E_1 and E_2 plates occurs about 15.6V and between E_4 and E_1 plates occurs about 7.3V.

Figures 5 (a) and 5 (b) show varactor capacitance variations with and without the fourth plate (E_4) respectively. As it was expected, adding the fourth plate has no effect on maximum capacitance value, but it decreases minimum capacitance value via increasing air gap between E_1 and E_2. The tuning range of the varactor's capacitance is presented here as:

$$\frac{C_{\max}-C_{\min}}{C_{\min}} = \frac{0.109-0.04214}{0.04214} = 1.587. \quad (5)$$

So, simulated varactor tuning range is 2.587:1, which is less than calculated theoretical value (3:1) due to fringing capacitance.
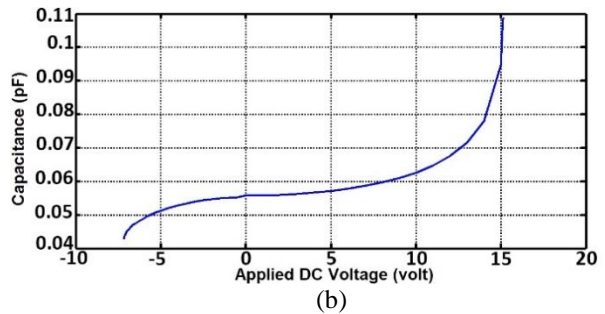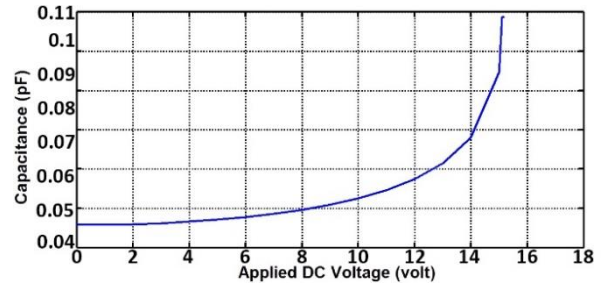

(a)

(b)

Fig. 5. The capacitance of the wide tuning range varactor vs. applied DC voltage: (a) without E4, and (b) with E4.

V. MICROWAVE SIMULATION

The RF behavior of the variable capacitor is simulated using HFSS software [12]. The simulated S_{11} parameter on smith chart is plotted from 1 GHz to 20 GHz, as shown in Fig. 6.

The calculated Q-factor is obtained as $1/\omega RC$. R and C are extracted by simulated S_{11} parameter, Fig. 6. The Q-factor of the proposed capacitor, from the simulated data at 10 GHz, is found to be 175. The Q-factor of the capacitor is shown in Fig. 7, over the frequency range 1-20 GHz.

Using S_{11} parameter calculated in HFSS, the linear equivalent circuit of the four-plate varactor can be presented as in Fig. 8, which offers a linear circuitry

model to describe the steady state behavior of varactor. $C5$, $L5$ and $R5$ represent plates E_1 and E_2. Coupling between the silicon substrate and the top plate is modeled by $C4$, $L4$ and R4. $C1$, $L1$, $L2$, and $R1$ are the capacitance, inductance and resistance associated with the attached supporting beams that are connected to the top plate. The anchors located around the varactor can be represented by $C2$ and $R2$. The inductance and the capacitance of the wires forming a connection between the center RF pad and the beams' anchors are represented by $C4$ and $L3$. Finally, $C3$ and $L3$ represent RF pads. These elements are determined by parameter extraction from the HFSS simulations at zero dc bias voltage [13]. As shown in Figs. 9 (a) and 9 (b), magnitude and phase of S_{11} calculated by linear circuitry model are in satisfying agreement with HFSS results.
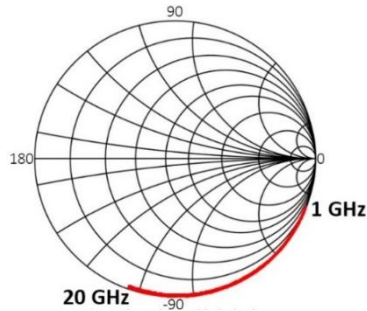

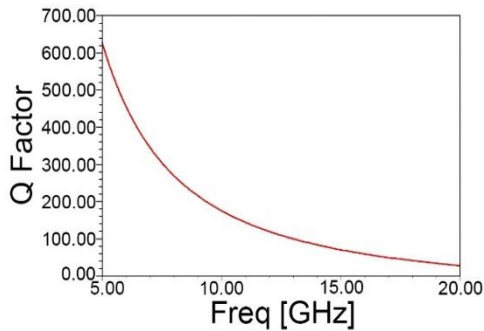Fig. 6. S_{11} parameter for four-plate varactor proposed in this paper.

Fig. 7. The quality factor for four-plate variable capacitor over frequency range from 1 GHz up to 20 GHz.
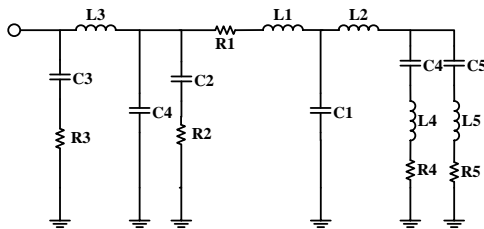

Fig. 8. The equivalent circuit of the simulated proposed varactor as a one-port network.
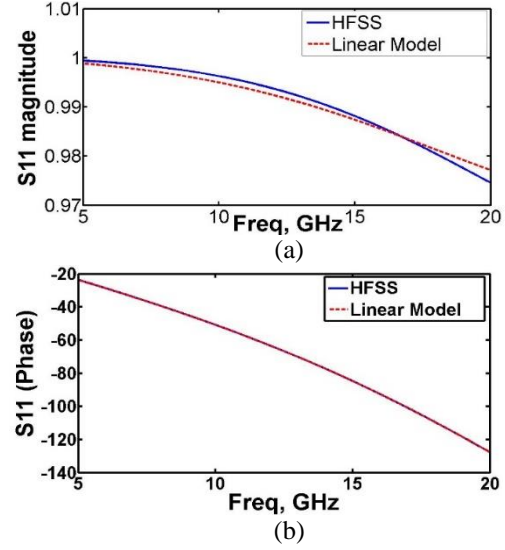

Fig. 9. The comparison between HFSS results and linear model results: (a) magnitude of S_{11} vs. frequency, and (b) phase of S_{11} vs. frequency.

VI. DYNAMIC ELECTROMECHANICAL SIMULATION (NONLINEAR CAD MODEL OF A MEMS VARACTOR)

A second-order system can mathematically describe the electromechanical dynamic behavior of the tunable capacitor [14]. In this second-order system viscous damping, inertia and spring force are considered as:

$$m\frac{d^2x}{dt^2} + b\frac{dx}{dt} + kx = f_{ext},\qquad(6)$$

where m is the mass of the movable plate E_1, b is the damping coefficient, the damping force (F_D) determined by bdx/dt, kx is the spring force and f_{ext} denotes the electrostatic force applied on E_1 which is calculated by Equation (2). The frequency response can be achieved by Fourier transferring of Equation (6):

$$\frac{X(j\omega)}{F(j\omega)} = \frac{1}{k}\left(\frac{1}{1-\left(\omega/\omega_0\right)^2 + j\omega/\left(Q\omega_0\right)}\right),\qquad(7)$$

where $\omega_0 = \sqrt{k/m}$ is the mechanical resonance frequency and $Q = k/\omega_0 b$ is the mechanical quality factor.

The squeezed air-film underneath the E_1 produces a damping force that opposes the downward motion of the E_1. The behavior of the squeezed air film between the closely spaced E_1 and the bottom plates is governed by Reynold's equation [15]:

$$\frac{\partial}{\partial x}\left[\left(\frac{\rho h^3}{\mu}\right)\frac{\partial P}{\partial x}\right] + \frac{\partial}{\partial y}\left[\left(\frac{\rho h^3}{\mu}\right)\frac{\partial P}{\partial y}\right] = 12\frac{\partial(\rho h)}{\partial t},\qquad(8)$$

where p denotes the pressure in the film, μ is the coefficient of the air viscosity, ρ is density, and h is the thickness of the air. The small geometry of the MEMS devices causes negligible temperature variation. Under isothermal condition, ρ is directly proportional to the P, and Reynold's equation is simplified as:

$$\frac{\partial}{\partial x}\left[\left(\frac{Ph^3}{\mu}\right)\frac{\partial P}{\partial x}\right]+\frac{\partial}{\partial y}\left[\left(\frac{Ph^3}{\mu}\right)\frac{\partial P}{\partial y}\right]=12\frac{\partial(Ph)}{\partial t}. \quad (9)$$

In order to determine the damping coefficient (b) in Equation (1), the simplified Reynold's equation is used by the COMSOL Multiphysics 3.5a. The simulated damping coefficient (b) is 1.38×10^{-4} kg/s. This damping coefficient leads to a settling time of 500 μsec. A specific pattern for perforating E_1, illustrated in Fig. 10, is used to reduce the settling time.

Equations (1), (2) and (7) are coupled together. These equations describe the relationship between the electrical and mechanical domain. Finite-difference method is used to solve these equations in MATLAB. A third order polynomial is used to fit capacitance as a function of the E_1's displacement. The simulated displacement of E_1 and varactor capacitance vs. time are shown in Fig. 11, when DC voltage of 8 volts is applied between E_1 and E_3. Perforating of E_1 results in damping coefficient of $b=5e^{-5}$. In downward motion, the squeezed film damping on E_1 is simulated by the COMSOL Multiphysics 3.5a, Fig. 10.
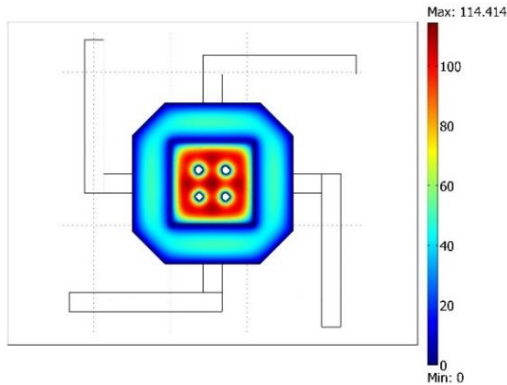

Fig. 10. The perforated E_1 plate in order to reach $b=5e^{-5}$ when V_{DC} is applied between E_1 and E_3.

As shown in Fig. 11, damping coefficient of $b=5e^{-5}$ leads to a settling time of 55 μsec.

In order to demonstrate the nonlinear behavior in circuits using MEMS varactors, a nonlinear model of the MEMS device is implemented, Fig. 12. Capacitance is modeled by module 3 that is calculated by Equation (1). The E_1's displacement is calculated from the electrostatic force by module 2 which uses Equation (6).

The electrostatic force is calculated by module 1 from voltage V_{DC} (module 3's output) and the

displacement x. This module generates an output voltage f equivalent to the electrostatic force, Equation (3). For implementing the nonlinear model described in Fig. 12, SDD tool is used from Agilent ADS, Fig. 13. Applying V_{DC} causes changing in the capacitance value (C). Using the concept of analogues systems, the value of C is calculated by the electrical system, Fig. 13. Following this, using SDD in ADS, the relation between current and voltage of the output port is defined as a capacitance.
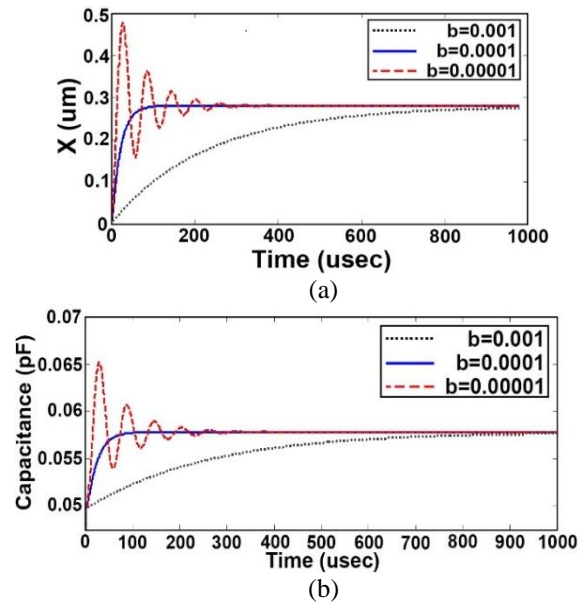

(a)

(b)

Fig. 11. The transient behavior of the proposed MEMS varactor at different damping coefficients: (a) E_1's displacement vs. time, and (b) the value of capacitance vs. time.
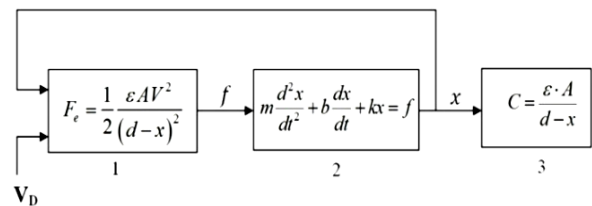

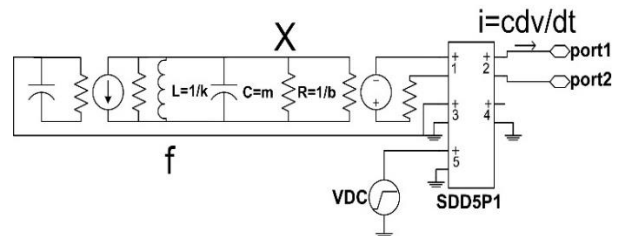Fig. 12. Modeling of the proposed MEMS varactor's nonlinear behavior.

Fig. 13. The nonlinear model for simulation of MEMS varactor's transient behavior.

The proposed four-plate MEMS varactor's response to a step voltage with rise time of 1 psec is obtained by using the nonlinear model, Fig. 14. Comparing the results of the nonlinear model with numerical solution, reveals that nonlinear model is not only reliable but also can help adequate modeling of the varactor's transient behavior. Furthermore, varacor variation via applying sawtooth voltage is shown in Fig. 15.
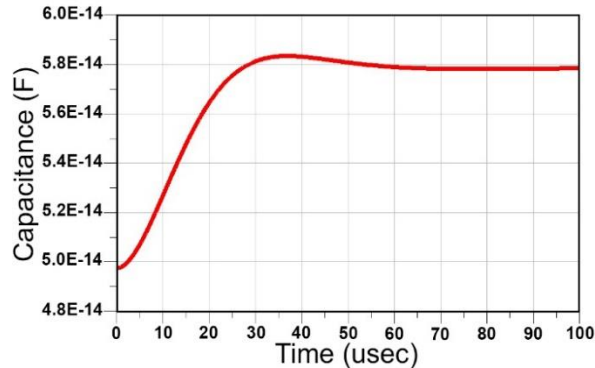

Fig. 14. The simulated capacitance vs. time when subject to a step voltage.
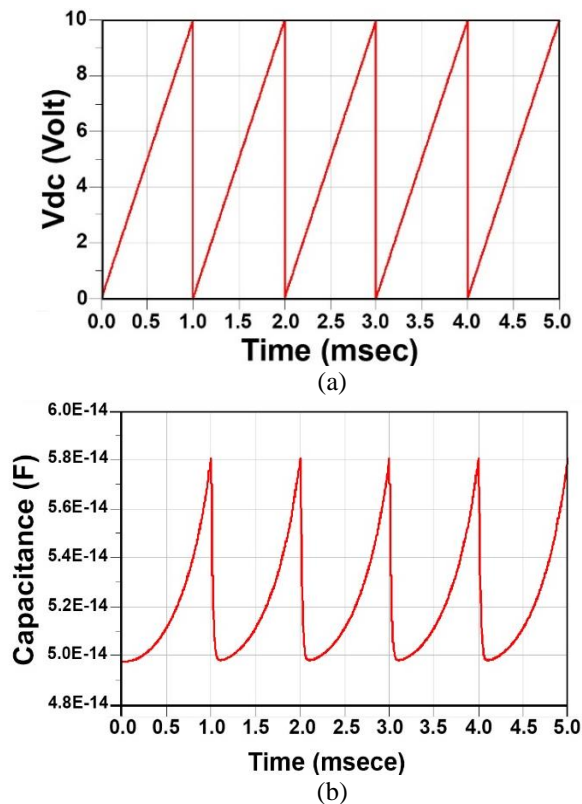

(a)

(b)

Fig. 15. (a) The sawtooth input voltage applied to the varactor as a tuning voltage. (b) The periodic response of the presented MEMS varactor to the periodic sawtooth input.

VII. CONCLUSION

In this paper, a high-Q varactor with wide tuning range was presented. This novel structure consists of four plates, two suspended plates and two fixed plates. The fourth plate was used to increase the distance between capacitance's plates in order to decrease the varactor's capacitance. Therefore, adding E_4 to three plate varactor led to the wider tuning range. The novel structure gained a tuning range of 2.587:1 (158.7%). Also, the proposed MEMS varactor in this paper showed a Q of 175 at 10 GHz.

Electromechanical behaviors of the varactor were also characterized. We studied both dynamic and static behaviors of the MEMS varactor. A perforated pattern for E_1 was chosen to achieve a proper damping coefficient leading to a fast transient behavior.

Microwave parameters were also studied by the simulation software. An equivalent circuit of the presented varactor was obtained by simulated S-parameters. The dynamic behavior of the varactor was modeled in this research work in order to study transient responses of the varactor.

REFERENCES

[1]   N. Nguyen and R. Meyer, "Si IC-compatible inductors and LC passive filters," *IEEE J. Solid-State Circuits*, vol. 25, pp. 1028-1031, Aug. 1990.

[2]   M. Soyuer, K. Jenkins, J. Burghartz, and M. Hulvey, "A 3 V 4 GHz nMOS voltage-controlled oscillator with integrated resonator," *IEEE ISSCC Dig. Tech. Papers*, pp. 394-395, Feb. 1996.

[3]   D. J. Young and B. E. Boser, "A micro-machined variable capacitor for monolithic low-noise VCOs," *IEEE Solid-State Sensor and Actuator Workshop Dig.*, pp. 86-89, June 1996.

[4]   A. Dec and K. Suyana, "Micromachined varactor with a wide tuning range," *Electronics Letters*, vol. 33, no. 11, pp. 922-924, May 1997.

[5]   A. Dec and K. Suyana, "Micromachined capacitors and their application to RF IC's," *IEEE Transactions on Microwave Theory and Techniques*, vol. 46, no. 12, pp. 2587-2596, 1998.

[6]   A. Dec and K. Suyana, "2.4 GHz CMOS LC VCO using micromachined variable capacitors for frequency tuning," *Microwave Symposium Dig.*, 1999 IEEE MTT-S International, vol. 1, pp. 79-82, 1999.

[7]   T. Clark, C. Nguyen, L. P. B. Katehi, and G. M. Rebeiz, "Micromachined devices for wireless communications," *Proceeding of the IEEE*, vol. 86, no. 8, pp. 1756-1767, 1998.

[8]   E. Abbaspour-Sani, N. Nasirzadeh, and G.

Dadashzadeh, "Two novel structures for tunable MEMS capacitor with RF applications," *Progress In Electromagnetics, PIER 68*, pp. 169-183, 2007.

[9] M. Zahn, *Electromagnetic Field Theory: A Problem Solving Approach*, John Wiley & Sons, New York, 1979.

[10] G. M. Rebeiz, *RF MEMS Theory, Design, and Technology*, John Wiley & Sons, 2003.

[11] J. Chen, J. Zou, C. Liu, J. E. Schutt-Ainé, S.-M. K. Kang, "Design and modeling of a micromachined high-Q tunable capacitor with large tuning range and a vertical planar spiral inductor," *IEEE Transactions on Eelectron Devices*, vol. 59, no. 3, pp. 730-739, Mar. 2003.

[12] Ansoft High Frequency Structure Simulation (HFSS), ver. 11, Ansoft Corporation, Pittsburgh, PA, 2005.

[13] M. Bakri-Kassem, Novel RF MEMS Varactors Realized in Standard MEMS and CMOS Processes, *Doctoral Dissertation, University of Waterloo*, Ontario, Canada, 2007.

[14] W. Weaver, Jr., S. P. Timoshenko, and D. H. Young, *Vibration Problems in Engineering*, John Wiley & Sons, New York, 1990.

[15] W. A. Gross, L. A. Matsch, V. Castelli, A. Eshel, J. H. Vohr, and M. Wildmann, *Fluid Film Lubrication*, John Wiley & Sons, New York, 1980.

[16] S. Lakshmi, S. Rao, P. Manohar, and P. N. Sayanu, "Design and simulation of multi-beam RF MEMS varactor," *Circuits, Communication, Control and Computing (I4C), International Conference on*, vol. 1, pp. 308-311, Nov. 2014.

Reze Sarraf Shirazi received the B.S., M.S., and Ph.D. degrees from the Amirkabir University of Technology (Tehran Polytechnic), Iran, in 1980, 1993, and 2006, respectively. He is currently an Associate Professor at the Amirkabir University of Technology, where he is Director of the Wave Propagation & Microwave Measurement Lab.

His interest fields are wave propagation, numerical methods in electromagnetic and radio link design. In addition, he has published two papers in ACES Journal.

Abdolali Abdipour received the B.S. from University of Tehran, Iran, in 1988, and M.S. degree from University of Limoges, France, 1992. He received the Ph.D. degree from the University of Paris XI(Orsay), France, 1996. He is currently a Professor at the Amirkabir University of Technology. He is currently the Director of Institute of Communication Technology and Applied Electromagnetic at Amirkabir University of Technology, 2012-Present.

His research interests include RF/Microwave/Millimeter-Wave/THz Circuits and Systems Design, and Linear and Nonlinear Modeling of Microwave/Millimeter-wave Circuits and Devices. In addition, he has published two papers in ACES Journal.

Mehrdad Moradi received the B.S. degree from the Isfahan University of Technology, Iran, and the M.S. degree from the Tehran Polytechnic, Iran, in 2008 and 2011, respectively. He is currently Faculty Member of the Islamic Azad University, Iran. His major research interest lines in the RF MEMS devices and their application. In addition, RF and microwave circuits and applied electromagnetics are his research interests.